

VisualGPT: Data-efficient Adaptation of Pretrained Language Models for Image Captioning

Jun Chen¹ Han Guo² Kai Yi¹ Boyang Li³ Mohamed Elhoseiny¹

¹King Abdullah University of Science and Technology

²Carnegie Mellon University ³Nanyang Technological University

{jun.chen, kai.yi, mohamed.elhoseiny}@kaust.edu.sa

hanguo@cs.cmu.edu, boyang.li@ntu.edu.sg

Abstract

The ability to quickly learn from a small quantity of training data widens the range of machine learning applications. In this paper, we propose a data-efficient image captioning model, VisualGPT, which leverages the linguistic knowledge from a large pretrained language model (LM). A crucial challenge is to balance between the use of visual information in the image and prior linguistic knowledge acquired from pretraining. We designed a novel self-resurrecting encoder-decoder attention mechanism to quickly adapt the pretrained LM as the language decoder on a small amount of in-domain training data. The proposed self-resurrecting activation unit produces sparse activations but has reduced susceptibility to zero gradients. We train the proposed model, VisualGPT, on 0.1%, 0.5% and 1% of MSCOCO [50] and Conceptual Captions [74] training data. Under these conditions, we outperform the best baseline model by up to 10.8% CIDEr on MS COCO and up to 5.4% CIDEr on Conceptual Captions. Further, VisualGPT achieves the state-of-the-art result on IU X-ray [19], a medical report generation dataset. To the best of our knowledge, this is the first work that improves data efficiency of image captioning by utilizing LM pretrained on unimodal data. Our code is available at: <https://github.com/Vision-CAIR/VisualGPT>.

1. Introduction

Image captioning [38, 85, 33, 17, 29] is a prominent example of cross-modal reasoning, requiring accurate understanding of the visual content and precise expression of that understanding in natural language. In addition to its scientific value, the task finds practical applications such as facilitating people with impaired vision [7, 11] and generating medical imaging reports under human supervision [47, 10].

Recent performance gains in image captioning mostly

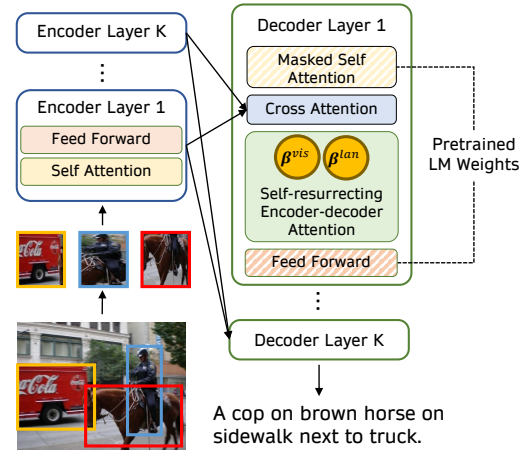


Figure 1. Our VisualGPT model transfers the knowledge from a pretrained language model to the caption decoder. A self-resurrecting encoder-decoder attention is designed to connect the multi-level visual features and caption decoder.

rely on large-scale image-caption corpora such as MS COCO [50] or Conceptual Captions [74], each containing more than one million captions. Manually creating these captions requires considerable time and effort. On the other hand, semi-automatic approaches for collecting image-caption pairs from the Internet, as used by Conceptual Captions [74], may generate incorrect or undesirable training data even after multiple rounds of data cleaning; data crawled from the Internet are unlikely to cover highly specific domains such as X-ray images [19]. Thus, the availability of training data limits the range of imagery that neural networks can reliably describe [1]. Improving the data efficiency thus will allow quick data curation and creation of systems that can describe rare objects in specific domains.

In this paper, we investigate the data efficiency problem for image captioning. This problem is distinct from the novel object captioning problem [28, 1], which relies

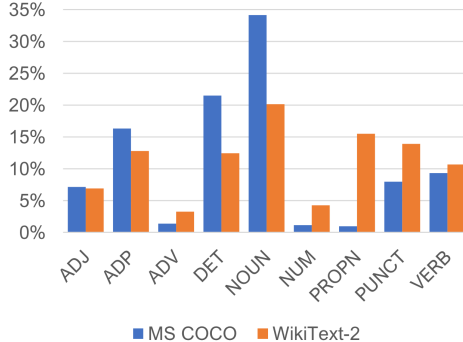


Figure 2. Comparison of the part-of-speech distributions of the MS COCO and WikiText-2 datasets [59]. We use the spacy parser and show only the most important categories.

on abundant in-domain data but zero out-of-domain data. Instead, we aim to improve the performance of image captioning systems trained on a small subset of *in-domain* data.

We propose to improve data efficiency by leveraging pretrained language models (LMs) [22, 53, 41, 67], such as BERT [20], XLNet [87], and GPT [65, 66, 8]. Via self-supervised learning, these models acquire rich linguistic and semantic knowledge, which has been shown to inform downstream tasks in NLP [9, 25]. However, few work address the adaptation of LMs pretrained on unimodal textual data for multimodal tasks.

A challenge in utilizing pretrained LMs is to bridge the gap between multi-modal tasks and the single-modal textual data the LMs are pretrained on. In Figure 2, we compare the part-of-speech distributions of MS COCO and WikiText-2 [59]. MS COCO employs 75% more nouns but 14% fewer verbs. This suggests that the MS COCO captions are biased toward descriptions of static objects rather than actions. As a result, effective use of pretrained LMs in image captioning requires careful balancing of the linguistic knowledge acquired from pretraining and the visual input information.

Figure 1 shows the overall architecture of the proposed network, called VisualGPT. In the commonly used encoder-decoder architecture for image captioning, we initialize the parameters of the decoder from pretrained LMs such as GPT-2 [66], whereas the encoder layers are randomly initialized. In addition, we propose an attention mechanism with self-resurrecting activation units (SRAUs), which balances the input from the visual encoder and the linguistic input from the previous decoder layer. The proposed mechanism can produce sparse activations while not being as vulnerable to the zero-gradient problem as regular gates; the self-resurrecting gates can be “turned on” again after being zeroed out.

Empirical results demonstrate that, when trained on 0.1%, 0.5% and 1% of the MS COCO and Conceptual Captions data, VisualGPT outperforms several strong baseline models. We achieve the state-of-the-art result on IU X-ray

[19], a medical report generation dataset. With several ablation experiments, we verify the effectiveness of pretrained LMs and the proposed self-resurrecting attention mechanism.

With this paper, we make the following contributions:

- We propose to investigate the data efficiency problem for image captioning and to borrow weights from pretrained language models for the purpose of initializing the decoder. Using only a small amount of in-domain training data, the proposed encoder-decoder quickly adapts network weights obtained from the textual modality to the cross-modal task of image captioning. To our knowledge, this is the first work that focuses on efficiently adapting large pretrained language models for image captioning.
- We propose a novel encoder-decoder attention with self-resurrecting activation units (SRAUs), which can learn to balance features from the visual and textual modalities. SRAU produces sparse activations while not being easily “trapped” in a zero-gradient region.

2. Related Work

Image Captioning. Image captioning has been extensively studied in computer vision research. Early methods [23, 44, 76, 89, 38] focus on filling templates with extracted objects, attributes, and relationships. With the advent of deep learning, researchers proposed end-to-end neural networks that encode an image into vector representations and decode a caption word by word [36, 82, 21, 32]. Many improvements to the encoder [15, 85, 57, 90, 86, 91, 45], the decoder [88, 84, 83], and the attention mechanism [12, 40, 92, 43, 29, 17] has since been proposed. Encoding the image using object regions has proven beneficial [3]. Reinforcement learning enables model optimization with non-differentiable evaluation metrics [69, 52, 18, 75]. [16, 13] investigate fine-grained control of caption generation. [18, 75] adopt GAN-like architecture to make automatically generated captions similar to human captions.

A few formulations of the image captioning problem deviate from the traditional supervised learning paradigm. Novel object captioning aims to describe objects that do not exist in the training data [28, 81, 58, 48, 1]. Feng *et al.* [24] propose unsupervised captioning without using paired image-caption supervision. As the only other paper that focuses on learning efficiency, Kim *et al* [34] improve the data efficiency by learning from auxiliary unpaired image-caption data.

Self-supervised NLP Models. Self-supervised training of large neural networks on textual data proves to be an important technique in the creation of high-performance NLP

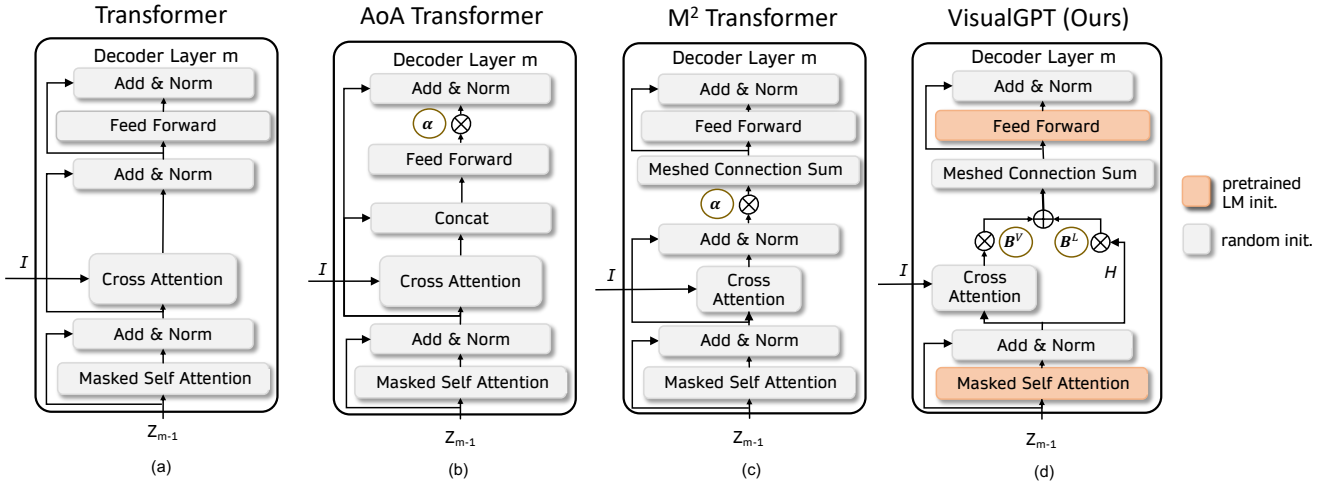


Figure 3. Architectures of vanilla Transformer [79], Transformer with AoA module [29] (AoA Transformer), \mathcal{M}^2 Transformer [17], and VisualGPT. We denote I and H as the visual and language features, respectively. Z_{m-1} is the output from decoder layer $m-1$. α , B^V and B^L represent different gating units.

models. Several self-supervision signals have been proposed, such as autoregressive language modeling [6, 60], which includes the GPT series of models [66, 8, 65], and masked language modeling, which includes ELMo [63] and BERT-related methods [20, 39, 54].

In this paper, we propose a quick adaptation technique for network weights obtained using the language modeling objective. However, the technique is not specific to this type of self-supervision signal and can be applied to other models, as the masked LM objective can be easily converted to the LM objective by masking only the last word in the textual sequence. Unlike neural networks pretrained on multimodal data (e.g., [64, 78, 77, 56, 46]), our method only requires a small amount of multimodal training data and focuses on adapting linguistic knowledge learned from the textual modality.

3. Background on Transformer

The Transformer [79] has become one of the standard models for image captioning. At its core is the self-attention mechanism and the encoder-decoder attention in the decoder. Given three matrices, the query Q , the key K , and the value V , the attention function is

$$\text{Attn}(Q, K, V) = \text{softmax} \left(\frac{(W^q Q)(W^k K)^\top}{\sqrt{D}} \right) W^v V, \quad (1)$$

where W^q , W^k , and W^v are trainable parameters and D is a scaling factor. Intuitively, the attention operation can be seen as encoding $W^q Q$ as convex combination of the row vectors of $W^v V$. The multi-head version adopts more than one sets of W^q , W^k , and W^v ; the results are concatenated and linearly projected back to the same dimensionality.

In the encoder-decoder attention, we have the encoder output $I \in \mathbb{R}^{O \times S}$ and the current state of the decoder $H \in \mathbb{R}^{t \times S}$. Here O is the input sequence length, S is the hidden dimension, and t the number of tokens already decoded. We use H as the query and I as both the key and the value. The encoder-decoder attention can be written as

$$\text{EncDecAttn}(H, I) = \text{Attn}(H, I, I). \quad (2)$$

After that, we apply the AddNorm operator, which contains a residual connection and layer normalization [4] and can be written as

$$\text{LayerNorm}(\text{EncDecAttn}(H, I) + H). \quad (3)$$

In conventional encoder-decoder transformers, only the output of the last encoder layer is used. In \mathcal{M}^2 Transformer [17], the output of all encoder layers go through the same encoder-decoder attention. The results from different encoder layers are multiplied by a set of gates and summed. The Attention-on-Attention (AoA) module [29] can be used to fuse the visual and linguistic information after cross-attention. We contrast these decoder architectures with VisualGPT in Figure 3.

4. VisualGPT

Pretrained language models such as GPT-2 [66] do not have encoder-decoder attention modules. When adapting such LMs to the task of image captioning, we need to insert the encoder-decoder attention into the pretrained model. This introduces the need to balance the pretrained weights, which have been optimized under a different data distribution, with the randomly initialized weights, which will be trained from scratch. In addition, the image captioning task

requires the conciliation of information from two different modalities.

The issue of balance can be intuitively understood from the perspective of visual vs. linguistic knowledge. We hypothesize that the generation of visual words, such as “person”, “truck”, or “dog”, requires the model to rely on visual information. In contrast, the generation of determiners or connectives requires only linguistic knowledge. Ideally, we would like to exploit the massive amount of linguistic knowledge stored in the pretrained LM weights [51], while referring to the visual input only when required. To achieve this goal, we introduce a pair of specialized gates.

4.1. Self-Resurrecting Activation Unit

$\text{EncDecAttn}(H, I)$ may be seen as encoding the linguistic information H with visual information I . In VisualGPT, we control the balance between these two modalities using two complementary gates B^{vis} and B^{lan} instead of AddNorm. The output of this module is

$$B^{\text{vis}} \otimes \text{EncDecAttn}(H, I) + B^{\text{lan}} \otimes H, \quad (4)$$

where \otimes denotes element-wise multiplication. Letting $B^{\text{vis}}[i, j]$ and $B^{\text{lan}}[i, j]$ denote the elements in the matrices, they are computed in pairs as

$$\begin{aligned} B^{\text{vis}}[i, j] &= \sigma(H[i, j]) \mathbb{1}(\sigma(H[i, j]) > \tau), \\ B^{\text{lan}}[i, j] &= (1 - \sigma(H[i, j])) \mathbb{1}(1 - \sigma(H[i, j]) > \tau). \end{aligned} \quad (5)$$

where τ is a predefined threshold hyperparameter and $\mathbb{1}(\cdot)$ is the indicator function, which returns 1 if the inner statement is true and 0 otherwise.

The indicator functions $\mathbb{1}(\sigma(\alpha) > \tau)$ and $\mathbb{1}(1 - \sigma(\alpha) > \tau)$ set the SRAUs apart from regular gates, which are computed simply as $\sigma(H[i, j])$ and $1 - \sigma(H[i, j])$. When τ is set to 0, SRAU becomes regular complementary gates. The thresholding introduces sparsity by setting some gates directly to zero. Figure 4 (left) visualizes the SRAU function.

In ordinary complementary gates, when the output of one gate is nearly zero, the output of the other gate is nearly one, and the gradients of both diminish. Hence, it is difficult for gradient descent to change gates in such states.

In SRAU, however, it is possible for one gate to output zero and have zero gradient while the gradient for the other gate remains usable (e.g., when x is close to 1.3 or -1.3). The asymmetry allows gradient-based optimization to effectively change the zero-outputting gate by changing $H[i, j]$ through the other gate. For this reason, we name these gates self-resurrecting activation units.

We further contrast SRAU with a “normalized” version,

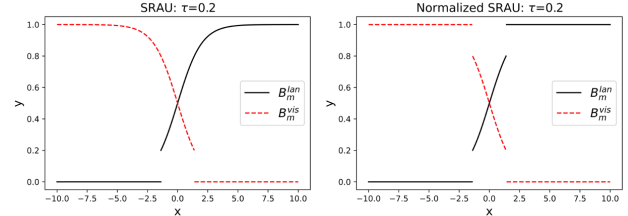


Figure 4. Left: Self-resurrecting activation function with $\tau = 0.2$. Right: Normalized self-resurrecting activation. The x-axis indicates the function inputs and the y-axis indicates function values.

denoted as $\tilde{B}^{\text{vis}}[i, j]$ and $\tilde{B}^{\text{lan}}[i, j]$,

$$\begin{aligned} \tilde{B}^{\text{vis}}[i, j] &= \frac{B^{\text{vis}}[i, j]}{B^{\text{vis}}[i, j] + B^{\text{lan}}[i, j]}, \\ \tilde{B}^{\text{lan}}[i, j] &= \frac{B^{\text{lan}}[i, j]}{B^{\text{vis}}[i, j] + B^{\text{lan}}[i, j]}. \end{aligned} \quad (6)$$

which are illustrated in Figure 4 (right). Like regular complementary gates, the normalized version always sum to one, but loses the asymmetry that enables the self-resurrecting property. In the ablation experiments (Section 5.4), we show that SRAU outperforms both regular complementary gates and normalized SRAU.

4.2. The Architecture and Training of VisualGPT

For completeness, we introduce the overall architecture for VisualGPT. The image encoder comprising K Transformer layers. Given an image, we extract objects in the image using an off-the-shelf object detection network. After that, we feed the spatial location into the image encoder. As such, the image encoder outputs I of dimension $S \times O \times K$.

The caption decoder contains M layers and its parameters are initialized from a pretrained LM. We insert the encoder-decoder module, which is randomly initialized. We also apply meshed connections between the encoder and the decoder like in M^2 Transformer. The network is trained to maximize the probability of the next token w_t conditioned on the preceding tokens w_1, \dots, w_{t-1} and the encoder output I using the cross-entropy loss. After a predefined number of epochs on supervised learning, we switch to self-critical reinforcement learning [69] with CIDEr as the reward.

5. Experiments

5.1. Datasets and Evaluation Metrics

We evaluate our model on three datasets, MS COCO [50], Conceptual Captions [74], and IU X-ray [19]. MS COCO contains 123,287 images and each of them is annotated with 5 different captions. We follow the Karpathy split [33] for the validation and test set. The Conceptual Captions

Method	Decoder Layers	BLEU-1	BLEU-4	METEOR	ROUGE	CIDEr	SPICE
0.1% training data							
Transformer [79]	3	57.4 \pm 0.26	13.1 \pm 0.15	16.7 \pm 0.25	40.7 \pm 0.17	40.8 \pm 0.15	10.3 \pm 0.15
\mathcal{M}^2 Transformer [17]	3	56.9 \pm 0.14	13.1 \pm 0.21	16.9 \pm 0.09	40.6 \pm 0.24	40.9 \pm 0.89	10.2 \pm 0.10
AoA Transformer	3	56.6 \pm 1.85	13.5 \pm 1.81	15.9 \pm 0.36	40.7 \pm 1.04	38.4 \pm 4.30	9.9 \pm 0.58
Transformer [79]	12	44.0 \pm 2.35	3.8 \pm 0.44	9.5 \pm 0.40	36.0 \pm 3.15	4.74 \pm 1.10	2.1 \pm 0.15
\mathcal{M}^2 Transformer [17]	12	52.0 \pm 1.85	9.1 \pm 0.31	13.7 \pm 3.03	39.5 \pm 1.30	33.1 \pm 1.00	7.8 \pm 0.21
AoA Transformer	12	20.7 \pm 2.49	2.0 \pm 2.65	7.9 \pm 1.56	34.0 \pm 2.98	7.0 \pm 1.34	3.2 \pm 0.49
VisualGPT (τ =0)	12	57.9 \pm 2.40	15.7 \pm 0.50	17.1 \pm 0.11	41.4 \pm 0.28	44.3 \pm 1.50	10.7 \pm 0.15
VisualGPT (τ =0.2)	12	58.2\pm2.30	16.4\pm0.65	18.5\pm1.85	41.9\pm0.17	45.1\pm1.90	10.9\pm0.40
0.5% training data							
Transformer	3	62.8 \pm 0.45	18.8 \pm 0.64	19.4 \pm 0.20	45.2 \pm 0.57	59.2 \pm 0.41	13.0 \pm 0.15
\mathcal{M}^2 Transformer	3	63.3 \pm 0.10	19.4 \pm 0.42	19.8 \pm 0.27	45.6 \pm 0.12	61.3 \pm 0.75	13.7 \pm 0.22
AoA Transformer	3	63.5 \pm 1.25	20.2 \pm 1.56	19.4 \pm 0.31	45.8 \pm 0.60	63.9 \pm 4.30	13.8 \pm 0.60
Transformer	12	60.9 \pm 0.34	15.8 \pm 0.29	18.0 \pm 0.12	43.1 \pm 0.25	49.7 \pm 1.04	11.0 \pm 0.08
\mathcal{M}^2 Transformer	12	60.1 \pm 1.38	14.4 \pm 0.10	17.9 \pm 0.72	43.7 \pm 0.86	44.2 \pm 0.30	11.4 \pm 0.26
AoA Transformer	12	57.9 \pm 2.62	15.5 \pm 0.71	17.1 \pm 0.42	43.4 \pm 0.28	46.8 \pm 1.13	11.3 \pm 0.21
VisualGPT (τ =0)	12	65.7 \pm 0.96	21.7 \pm 0.89	20.8 \pm 0.21	47.1 \pm 0.56	69.0 \pm 1.35	14.3 \pm 0.32
VisualGPT (τ =0.2)	12	66.2\pm1.19	22.1\pm0.96	21.1\pm0.40	47.3\pm0.61	70.3\pm1.70	14.6\pm0.25
1% training data							
Transformer	3	66.0 \pm 0.34	21.9 \pm 0.21	21.1 \pm 0.15	47.3 \pm 0.50	71.9 \pm 1.19	14.5 \pm 0.15
\mathcal{M}^2 Transformer	3	67.1 \pm 0.58	23.4 \pm 0.42	21.3 \pm 0.17	48.3 \pm 0.26	73.0 \pm 1.00	14.9 \pm 0.13
AoA Transformer	3	67.6 \pm 0.71	23.6 \pm 1.43	21.5 \pm 0.31	48.4 \pm 0.28	75.5 \pm 2.30	15.1 \pm 0.32
Transformer	12	64.0 \pm 0.56	19.6 \pm 0.83	19.5 \pm 0.22	45.7 \pm 0.49	62.1 \pm 0.67	12.5 \pm 0.17
\mathcal{M}^2 Transformer	12	63.3 \pm 1.28	18.0 \pm 0.62	19.3 \pm 0.64	46.1 \pm 0.85	52.9 \pm 5.00	12.7 \pm 0.55
AoA Transformer	12	63.7 \pm 0.92	17.7 \pm 0.14	18.5 \pm 0.14	48.2 \pm 2.12	58.4 \pm 0.57	12.5 \pm 0.64
VisualGPT (τ =0)	12	69.7\pm0.62	25.7\pm0.72	22.6\pm0.21	49.8\pm0.21	82.5\pm1.81	15.8 \pm 0.21
VisualGPT (τ =0.3)	12	69.3 \pm 0.84	25.2 \pm 1.11	22.6\pm0.20	49.6 \pm 0.46	81.7 \pm 2.70	16.0\pm0.25

Table 1. Performance of the compared methods training on 0.1%, 0.5% and 1% of MS COCO image-caption pairs. The best performance in each configuration is in bold.

dataset [74] contains a wider variety of both images and image caption styles than MS COCO. It contains around 3.3M images for training and 28K for validation. As the test data is not publicly available, we instead use the public validation data as our test set, and randomly sample 5000 different image-caption pairs from the training set as the validation set. All the sentences have been converted to lower cases. To create the small training data setup for MS COCO and Conceptual Captions, we randomly sample 0.1%, 0.5% and 1% image-caption pairs as training data. The procedure is repeated 4 times with different random seeds.

IU X-ray [19] is a radiography dataset containing 7,470 chest X-ray images and 3,955 human-written reports. As the dataset is already small, we follow the original split, which has a training set of 5,226 images and 2,770 reports. Most images have two images corresponding to the frontal and lateral viewpoint respectively.

The evaluation metrics include BLEU [61], METEOR

[5], ROUGE[49], CIDEr [80] and SPICE [2]. We report the average performance with standard deviation.

5.2. Experimental Settings

Baselines. We compare our model with several state-of-the-art transformer-based models, including (1) Plain Transformer [79] model. (2) **AoA Transformer**, which inserts an attention-on-attention (AoA) module [29] into every transformer layer, as depicted by Figure 3 (b). Following [17], we slightly update the original AoA network in [29] by replacing the LSTM with Transformers in order to create a fair Transformer-to-Transformer comparison. (3) \mathcal{M}^2 Transformer [17], the current state-of-the-art image-captioning model on MS COCO. As VisualGPT has 12 decoder layers, for fair comparisons, we also create variants of Transformer and \mathcal{M}^2 Transformer with 12-layer decoders. For VisualGPT, we tune the hyperparameter τ on the validation set and report results from the best performing τ .

Models	Decoder Layers	B-1	B-4	M	R	C
0.1% training data						
Transformer	3	12.4	2.4	4.9	15.2	21.2
\mathcal{M}^2 Transformer	3	13.1	2.8	4.8	15.5	23.5
AoA Transformer	3	11.4	2.4	4.6	14.7	20.9
VisualGPT ($\tau=0$)	12	14.0	3.2	5.4	16.2	27.2
VisualGPT ($\tau=0.2$)	12	13.9	3.2	5.6	16.7	27.7
0.5% training data						
Transformer	3	13.2	3.3	5.5	16.3	29.6
\mathcal{M}^2 Transformer	3	14.5	3.6	6.0	17.1	32.0
AoA Transformer	3	13.8	3.3	5.6	17.9	31.8
VisualGPT ($\tau=0$)	12	15.1	4.0	6.4	18.2	36.9
VisualGPT ($\tau=0.1$)	12	15.4	4.1	6.6	18.4	37.4
1% training data						
Transformer	3	13.9	3.7	6.3	18.1	37.9
\mathcal{M}^2 Transformer	3	16.0	4.1	6.8	18.9	39.8
AoA Transformer	3	14.9	4.1	6.5	18.6	39.0
VisualGPT ($\tau=0$)	12	15.0	4.1	6.6	18.2	40.0
VisualGPT ($\tau=0.1$)	12	16.4	4.3	6.9	19.2	41.2

Table 2. Performance of models trained on small subsets of Conceptual Captions.

Models	B-1	B-2	B-3	B-4	R	M	C
Att2in [70]	22.4	12.9	8.9	6.8	30.8	-	29.7
CoAtt [31]	45.5	28.8	20.5	15.4	36.9	-	27.7
HRGR [42]	43.8	29.8	20.8	15.1	32.2	-	34.3
CMAS-RL [30]	46.4	30.1	21.0	15.4	37.1	-	27.5
Chen <i>et al.</i> [14]	47.0	30.4	21.9	16.5	37.1	18.7	-
Ours ($\tau=0$)	47.7	30.9	21.9	15.5	34.8	20.1	45.6
Ours ($\tau=0.3$)	48.2	31.4	22.1	15.8	37.5	20.4	49.7

Table 3. Performance on the IU X-ray dataset.

We find τ in the range of $[0.1, 0.3]$ to offer the right level of sparsity. For all other baselines, we tune the hyperparameters on the validation set of MS COCO. Please see the supplemental material for more details on hyperparameters and experimental results.

5.3. Quantitative Results

Small In-domain Training Data. Results on MS COCO and Conceptual Captions are presented in Tables 1 and 2 respectively. On MS COCO, VisualGPT achieves the best performance among all models. VisualGPT outperforms the best baseline model by 4.2 CIDEr when trained on 0.1% of MS COCO data, 6.4 CIDEr with 0.5% data and 7.0 CIDEr with 1% data. In the experiments on the Conceptual Captions dataset, we compare against only baseline models utilizing 3-layer decoders as these baselines have demonstrated superior performance on MS COCO. Once again,

Models	B-1	B-4	M	R	C
Kim <i>et al.</i> [35]	58.1	13.4	15.9	-	36.0
Kim <i>et al.</i> + unpaired	63.0	18.7	20.7	-	55.2
VisualGPT ($\tau = 0$)	65.6	23.9	21.6	48.0	73.7
VisualGPT ($\tau = 0.2$)	67.1	24.3	21.9	48.6	75.8
Gu <i>et al.</i> [26]	46.2	5.4	13.2	-	17.7
Feng <i>et al.</i> [24]	58.9	18.6	17.9	-	54.9

Table 4. Comparison using Kim *et al.*’s split of MS COCO. Kim *et al.* employ only 1% images for training, whereas Kim *et al.* + unpaired also use the rest of training data as unpaired images and texts. We also include unsupervised baselines of Gu *et al.* and Feng *et al.*

VisualGPT outperforms all the baselines in every matrix evaluation. It outperforms the best baseline model by 4.2 CIDEr under 0.1% training data, 5.4 CIDEr under 0.5% data and 1.4 CIDEr under 1% data.

Medical Report Generation. We compared VisualGPT against state-of-the-art medical report generation models including Att2in [69], CoAtt [31], HRGR [42], CMAS-RL [30] and the model from Chen *et al.* [14]. This dataset only contains around 2,770 medical reports in the training set, which is less than 1% COCO data and poses a data-efficiency challenge. We follow the same experimental setting as in [14]. The results show that VisualGPT outperforms the baselines for most evaluation metrics.

Comparison against Semi-supervised and Unsupervised Methods. Kim *et al.* [35] proposed a semi-supervised learning method to improve the data efficiency of image captioning. They used 1% of images as training data, rather than 1% of image-caption pairs in Table 1. For Kim *et al.* + unpaired, they also employ the other 99% of MS COCO as unpaired images and captions for training. We replicate their setup. In Table 4, we compare VisualGPT against the results reported in [35]. Without using unpaired images and captions, the proposed VisualGPT method outperforms Kim *et al.* by 20.6 CIDEr score.

We also compared VisualGPT against unsupervised methods of Gu *et al.* [26] and Feng *et al.* [24], which use tens of millions of unpaired images and captions. Even though these are not fair comparisons, it is encouraging to see that only 1133 training images are needed to surpass their performance.

5.4. Ablation Studies

To measure the effects of random initialization and pre-trained GPT-2 weights with the following ablated versions of VisualGPT.

- **Random init.** The base model is a Transformer [79]

Ablation	B-1	B-4	M	R	C	S
0.1% COCO training						
Random init.	44.0	3.8	9.5	36.0	4.7	2.1
GPT2 init.	56.8	15.3	17.0	41.2	42.9	10.5
GPT2 init. + Meshed	54.9	14.7	16.6	41.1	41	10.4
GPT2 init. + AoA	55.5	14.4	16.2	40.7	40.1	10.2
Normalized SRAU	55.7	15.0	16.8	41.2	42.4	10.4
Full VisualGPT	58.2	16.4	18.5	41.9	45.1	10.9
0.5% COCO training						
Random init.	60.9	15.8	18.0	43.1	49.7	11.0
GPT2 init.	65.1	21.8	20.6	46.6	69.5	14.1
GPT2 init. + Meshed	64.7	21.8	20.7	47.1	68.5	14.2
GPT2 init. + AoA	64.2	21.2	20.5	46.5	67.2	13.8
Normalized SRAU	65.3	21.8	20.9	47.0	69.3	14.1
Full VisualGPT	66.2	22.1	21.1	47.3	70.3	14.6
1% COCO training						
Random init.	64.0	19.6	19.5	45.7	62.1	12.5
GPT2 init.	68.5	25.1	22.1	49.0	80.5	15.4
GPT2 init. + Meshed	68.2	25.0	22.4	49.2	80.4	15.4
GPT2 init. + AoA	68.5	24.6	22.0	48.6	78.4	15.0
Normalized SRAU	69.1	25.2	22.3	49.3	81.4	15.5
Full VisualGPT	69.7	25.7	22.6	49.8	82.5	15.8

Table 5. Ablation studies on VisualGPT with different initialization, different cross-attention mechanisms, and variants of SRAU gates, trained on MS COCO subsets.

architecture with a 3-layer encoder, a 12-layer decoder, and vanilla cross-attention between the encoder and the decoder. The model parameters are randomly initialized.

- **GPT2 init.** On top of the base model, we load the GPT-2 pretrained weights into the decoder. Other weights remain randomly initialized.

Table 5 shows the results. Comparing Random initialization and GPT2 initialization, it is evident that the GPT-2 weights play a significant role in learning from small data. In particular, the gap between these two models is the most pronounced when training on the least data.

Since AoA [29] and \mathcal{M}^2 Transformer [17] both have their own gating and cross-modal attention mechanism, we directly compare these network structures with the proposed SRAU in the following ablations.

- **GPT2 init. + Meshed.** On top of the Base + GPT2 init. model, we apply the meshed cross-connection between the encoder and the decoder [17] instead of the traditional cross-modality attention.
- **GPT2 init. + AoA.** On top of the Base + GPT2 init.

Method	0.1% data	0.5% data	1% data
Transformer [79]	19.6%	19.2%	17.2%
AoA Transformer [29]	9.6%	19.2%	24.4%
\mathcal{M}^2 Transformer [17]	31.2%	23.6%	22.0%
VisualGPT	39.6%	38.0%	36.4%

Table 6. The percentage of votes received by VisualGPT and baseline models under different quantity of training data.

Q1. Does the caption miss things shown in the image?						
Answer	Ours	\mathcal{M}^2 Transformer	Transformer	AoA	GT	
No	719	624	633	621	973	
Yes	367	438	456	447	73	
No Rate	0.66	0.59	0.58	0.58	0.93	
Q2. Does the caption describe things not in the image?						
Answer	Ours	\mathcal{M}^2 Transformer	Transformer	AoA	GT	
No	720	692	633	655	448	
Yes	360	418	423	412	43	
No Rate	0.67	0.62	0.60	0.61	0.96	

Table 7. Human evaluation of object hallucination and omission. GT denotes the ground-truth captions.

model, we add Attention on Attention [29] to the simple cross-modality attention in the decoder.

The VisualGPT model achieves the best performance in all three setups, demonstrating the effectiveness of the proposed mechanism.

We also create an ablation called **Normalized SRAU**, where we replace the SRAU with the normalized SRAU (see Figure 4) and use GPT2 initialization. The normalized SRAU results in substantially lowered performance, decreasing CIDEr from Full VisualGPT by 2.7, 1.0, and 0.3 respectively on the three setups. This demonstrates that the self-resurrecting property is beneficial for learning from small data. We experimented with Leaky ReLU and GELU, which ameliorate zero gradients, but the training crashed due to the lack of upper limits for function values.

The comparison between SRAU and regular complementary gates has been shown between the conditions $\tau > 0$ and $\tau = 0$ in Tables 1 through 4. We observe that VisualGPT consistently performs better when $\tau > 0$, indicating the benefits of SRAU over regular complementary gates.

5.5. Human Study

In addition to automatic evaluation metrics, we conduct two human studies to further evaluate the quality of captions generated. In the first study, we asked human participants directly for preference over generated captions. We randomly selected 50 test images from the three setups of 0.1%, 0.5%, and 1% training data. For every image, we

generated one caption from VisualGPT and each of three high-performing baselines from Table 1, Transformer [79], \mathcal{M}^2 Transformer [17], and AoA Transformer [29], all with three decoder layers. Every image was evaluated by 5 different Turkers, who chose the caption which most accurately described the image content. We received 750 valid responses. The results are summarized in Table 6.

Overall, we observe that the captions generated by VisualGPT received the largest share of votes, 39.6% for the 0.1% split, 38.0% for the 0.5% split, 36.4% for the 1% split. For each training setup, we conducted Pearson’s Chi-square test [62], which shows the differences are statistical significant with $p < 0.05$ in all cases.

In the second study, we evaluate if using pretrained language models introduces excessive linguistic prior that could cause the known object hallucination problem [72]. From the models trained using 1% COCO data. We randomly sampled 250 images with the generated caption from each model. For each image, we asked 5 different participants if the caption (1) described non-existent objects or (2) missed objects existing in the image. To catch random clickers, we created 5 images with verified captions, so that the right answers were known to us. Participants who answered these questions wrongly were considered unreliable and removed from the results.

The results are in Table 7. Compared to the baselines, VisualGPT has less hallucination and higher coverage of objects. The study also finds that the ground-truth captions has the least amount of hallucination and highest coverage of objects in the image. This finding lends positive support to the validity of the experimental protocol.

5.6. Qualitative Analysis

In this section, we examine examples from the VisualGPT model trained on 1% of MS COCO. First, we show example captions generated by VisualGPT in Figure 5 and the associated B^{vis} at the last decoder layer. Note that for every word generated, we have a 768-dimensional visual gate vector, which is a slice of B^{vis} at different time steps. We take the mean of the gate vector as the visual score for that word. After that, we normalize the visual scores across the dataset to the $[0, 1]$ interval and highlight the words accordingly. Blue indicates high visual scores and red indicates low visual scores. We observe that, in agreement with our intuition, VisualGPT assigns high visual scores to words like “desk” and “snowy surface” and low visual scores to determiners and prepositions.

In Figure 6, we plot the distribution of B^{vis} and B^{lan} at every decoder layer as a box-and-whisker diagram. We also show the words with the highest and lowest visual scores, which are again in line with our expectations. Additionally, we observe that, going from layer 0 to layer 9, the decoder makes increasing use of visual information, but the upper-

Figure 5 displays four examples of generated captions and their visual scores. Each example includes an image, the ground truth (GT) caption, and the generated caption (Ours) with attention scores for each word.

- GT: the lady is sitting on the wood bench**

Ours	a	woman	sitting	on	a	bench	in	a	park
attention	0.7	0.78	0.82	0.76	0.8	0.96	0.8	0.69	0.85
- GT: a laptop with a keyboard and mouse are on this desk**

Ours	a	laptop	sitting	on	a	desk	with	a	mouse
attention	0.7	0.78	0.81	0.7	0.7	0.92	0.85	0.64	0.76
- GT: a cat is sitting in front of a television**

Ours	a	cat	is	sitting	in	front	of	a	television
attention	0.8	0.86	0.8	0.83	0.7	0.72	0.6	0.71	0.93
- GT: a number of people sitting on a snowy surface with skis**

Ours	a	couple	of	people	sitting	on	a	snowy	surface
attention	0.8	0.87	0.71	0.85	0.91	0.76	0.71	0.94	0.95

Figure 5. Visual scores of words in generated captions. We show the raw visual scores and highlight them according to normalized visual scores. High visual scores are in blue and low scores in red.

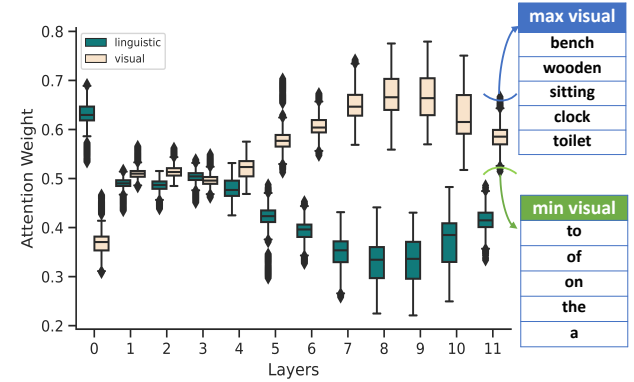


Figure 6. Distributions of linguistic attention (B^{lan}) and visual attention (B^{vis}) at every decoding layer. We also show the words generated with the highest and lowest visual attention.

most layers, 10 and 11, make more balanced use of information. We hypothesize that the low layers focus on low-level linguistics like syntax, whereas the middle layers learn to fuse linguistic information with visual information. Finally, the two information sources become balanced in the uppermost layers.

6. Conclusion

In this paper, we presented a data efficient image captioning model, VisualGPT, which leverages the linguistic knowledge from the pretrained language model. To bridge the semantic gap between different modalities, we designed a novel encoder-decoder attention mechanism with an unsaturated rectified gating function. We evaluate our model

on 0.1%, 0.5% and 1.0% of MS COCO and Conceptual Captions, and IU X-ray, a small medical imaging report dataset. We achieve the state-of-the-art result on IU X-ray and outperform several strong baseline models in other experiments.

References

- [1] Harsh Agrawal, Karan Desai, Yufei Wang, Xinlei Chen, Rishabh Jain, Mark Johnson, Dhruv Batra, Devi Parikh, Stefan Lee, and Peter Anderson. nocaps: novel object captioning at scale. In *Proceedings of the IEEE International Conference on Computer Vision*, pages 8948–8957, 2019. [1](#), [2](#)
- [2] Peter Anderson, Basura Fernando, Mark Johnson, and Stephen Gould. Spice: Semantic propositional image caption evaluation. In *European Conference on Computer Vision*, pages 382–398. Springer, 2016. [5](#)
- [3] Peter Anderson, Xiaodong He, Chris Buehler, Damien Teney, Mark Johnson, Stephen Gould, and Lei Zhang. Bottom-up and top-down attention for image captioning and visual question answering. In *Proceedings of the IEEE conference on computer vision and pattern recognition*, pages 6077–6086, 2018. [2](#), [13](#)
- [4] Jimmy Lei Ba, Jamie Ryan Kiros, and Geoffrey E. Hinton. Layer normalization. *arXiv 1607.06450*, 2016. [3](#)
- [5] Satanjeev Banerjee and Alon Lavie. Meteor: An automatic metric for mt evaluation with improved correlation with human judgments. In *Proceedings of the acl workshop on intrinsic and extrinsic evaluation measures for machine translation and/or summarization*, pages 65–72, 2005. [5](#)
- [6] Yoshua Bengio, Réjean Ducharme, Pascal Vincent, and Christian Jauvin. A neural probabilistic language model. *Journal of machine learning research*, 3(Feb):1137–1155, 2003. [3](#)
- [7] Jeffrey P. Bigham, Chandrika Jayant, Hanjie Ji, Greg Little, Andrew Miller, Robert C. Miller, Aubrey Tatarowicz, Brandyn White, Samuel White, and Tom Yeh. Vizwiz: Nearly real-time answers to visual questions. In *Proceedings of the 2010 International Cross Disciplinary Conference on Web Accessibility (W4A)*, 2010. [1](#)
- [8] Tom B Brown, Benjamin Mann, Nick Ryder, Melanie Subbiah, Jared Kaplan, Prafulla Dhariwal, Arvind Neelakantan, Pranav Shyam, Girish Sastry, Amanda Askell, et al. Language models are few-shot learners. *arXiv preprint arXiv:2005.14165*, 2020. [2](#), [3](#)
- [9] Paweł Budzianowski and Ivan Vulic. Hello, it’s GPT-2 - how can I help you? towards the use of pretrained language models for task-oriented dialogue systems. In Alexandra Birch, Andrew M. Finch, Hiroaki Hayashi, Ioannis Konstas, Thang Luong, Graham Neubig, Yusuke Oda, and Katsuhiro Sudoh, editors, *Proceedings of the 3rd Workshop on Neural Generation and Translation@EMNLP-IJCNLP 2019, Hong Kong, November 4, 2019*, pages 15–22. Association for Computational Linguistics, 2019. [2](#)
- [10] Aurelia Bustos, Antonio Pertusa, Jose-Maria Salinas, and Maria de la Iglesia-Vayá. Padchest: A large chest x-ray image dataset with multi-label annotated reports. *Medical image analysis*, 66, 2020. [1](#)
- [11] Prithvijit Chattopadhyay, Deshraj Yadav, Viraj Prabhu, Arjun Chandrasekaran, Abhishek Das, Stefan Lee, Dhruv Batra, and Devi Parikh. Evaluating visual conversational agents via cooperative human-ai games. In *HCOMP*, 2017. [1](#)
- [12] Long Chen, Hanwang Zhang, Jun Xiao, Liqiang Nie, Jian Shao, Wei Liu, and Tat-Seng Chua. Sca-cnn: Spatial and channel-wise attention in convolutional networks for image captioning. In *Proceedings of the IEEE conference on computer vision and pattern recognition*, pages 5659–5667, 2017. [2](#)
- [13] Shizhe Chen, Qin Jin, Peng Wang, and Qi Wu. Say as you wish: Fine-grained control of image caption generation with abstract scene graphs. In *Proceedings of the IEEE/CVF Conference on Computer Vision and Pattern Recognition*, pages 9962–9971, 2020. [2](#)
- [14] Zhihong Chen, Yan Song, Tsung-Hui Chang, and Xiang Wan. Generating radiology reports via memory-driven transformer. In *Proceedings of the 2020 Conference on Empirical Methods in Natural Language Processing (EMNLP)*, pages 1439–1449, 2020. [6](#)
- [15] Cesc Chunseong Park, Byeongchang Kim, and Gunhee Kim. Attend to you: Personalized image captioning with context sequence memory networks. In *Proceedings of the IEEE conference on computer vision and pattern recognition*, pages 895–903, 2017. [2](#)
- [16] Marcella Cornia, Lorenzo Baraldi, and Rita Cucchiara. Show, control and tell: A framework for generating controllable and grounded captions. In *Proceedings of the IEEE/CVF Conference on Computer Vision and Pattern Recognition*, pages 8307–8316, 2019. [2](#)
- [17] Marcella Cornia, Matteo Stefanini, Lorenzo Baraldi, and Rita Cucchiara. Meshed-memory transformer for image captioning. In *Proceedings of the IEEE/CVF Conference on Computer Vision and Pattern Recognition*, pages 10578–10587, 2020. [1](#), [2](#), [3](#), [5](#), [7](#), [8](#), [13](#), [14](#)
- [18] Bo Dai, Sanja Fidler, Raquel Urtasun, and Dahua Lin. Towards diverse and natural image descriptions via a conditional gan. In *Proceedings of the IEEE International Conference on Computer Vision*, pages 2970–2979, 2017. [2](#)
- [19] Dina Demner-Fushman, Marc D Kohli, Marc B Rosenman, Sonya E Shooshan, Laritza Rodriguez, Sameer Antani, George R Thoma, and Clement J McDonald. Preparing a collection of radiology examinations for distribution and retrieval. *Journal of the American Medical Informatics Association*, 23(2):304–310, 2016. [1](#), [2](#), [4](#), [5](#)
- [20] Jacob Devlin, Ming-Wei Chang, Kenton Lee, and Kristina Toutanova. Bert: Pre-training of deep bidirectional transformers for language understanding. In *Proceedings of the 2019 Conference of the North American Chapter of the Association for Computational Linguistics: Human Language Technologies, Volume 1 (Long and Short Papers)*, pages 4171–4186, 2019. [2](#), [3](#)
- [21] Jeffrey Donahue, Lisa Anne Hendricks, Sergio Guadarrama, Marcus Rohrbach, Subhashini Venugopalan, Kate Saenko, and Trevor Darrell. Long-term recurrent convolutional networks for visual recognition and description. In *Proceedings of the IEEE conference on computer vision and pattern recognition*, pages 2625–2634, 2015. [2](#)

[22] Li Dong, Nan Yang, Wenhui Wang, Furu Wei, Xiaodong Liu, Yu Wang, Jianfeng Gao, Ming Zhou, and Hsiao-Wuen Hon. Unified language model pre-training for natural language understanding and generation. In *Advances in Neural Information Processing Systems*, pages 13063–13075, 2019. 2

[23] Ali Farhadi, Mohsen Hejrati, Mohammad Amin Sadeghi, Peter Young, Cyrus Rashtchian, Julia Hockenmaier, and David Forsyth. Every picture tells a story: Generating sentences from images. In *European conference on computer vision*, pages 15–29. Springer, 2010. 2

[24] Yang Feng, Lin Ma, Wei Liu, and Jiebo Luo. Unsupervised image captioning. In *Proceedings of the IEEE conference on computer vision and pattern recognition*, pages 4125–4134, 2019. 2, 6

[25] Sergey Golovanov, Rauf Kurbanov, Sergey Nikolenko, Kyryl Truskovskyi, Alexander Tselousov, and Thomas Wolf. Large-scale transfer learning for natural language generation. In *Proceedings of the 57th Annual Meeting of the Association for Computational Linguistics*, pages 6053–6058, 2019. 2

[26] Jiuxiang Gu, Shafiq Joty, Jianfei Cai, and Gang Wang. Unpaired image captioning by language pivoting. In *Proceedings of the European Conference on Computer Vision (ECCV)*, pages 503–519, 2018. 6

[27] Kaiming He, Xiangyu Zhang, Shaoqing Ren, and Jian Sun. Deep residual learning for image recognition. In *Proceedings of the IEEE conference on computer vision and pattern recognition*, pages 770–778, 2016. 13

[28] Lisa Anne Hendricks, Subhashini Venugopalan, Marcus Rohrbach, Raymond Mooney, Kate Saenko, and Trevor Darrell. Deep compositional captioning: Describing novel object categories without paired training data. In *Proceedings of the IEEE conference on computer vision and pattern recognition*, pages 1–10, 2016. 1, 2

[29] Lun Huang, Wenmin Wang, Jie Chen, and Xiao-Yong Wei. Attention on attention for image captioning. In *Proceedings of the IEEE International Conference on Computer Vision*, pages 4634–4643, 2019. 1, 2, 3, 5, 7, 8, 14

[30] Baoyu Jing, Zeya Wang, and Eric Xing. Show, describe and conclude: On exploiting the structure information of chest x-ray reports. In *Proceedings of the 57th Annual Meeting of the Association for Computational Linguistics*, pages 6570–6580, 2019. 6

[31] Baoyu Jing, Pengtao Xie, and Eric Xing. On the automatic generation of medical imaging reports. In *Proceedings of the 56th Annual Meeting of the Association for Computational Linguistics (Volume 1: Long Papers)*, pages 2577–2586, 2018. 6

[32] Justin Johnson, Andrej Karpathy, and Li Fei-Fei. Densecap: Fully convolutional localization networks for dense captioning. In *Proceedings of the IEEE conference on computer vision and pattern recognition*, pages 4565–4574, 2016. 2

[33] Andrej Karpathy and Li Fei-Fei. Deep visual-semantic alignments for generating image descriptions. In *Proceedings of the IEEE conference on computer vision and pattern recognition*, pages 3128–3137, 2015. 1, 4

[34] Dong-Jin Kim, Jinsoo Choi, Tae-Hyun Oh, and In So Kweon. Image captioning with very scarce supervised data: Adversarial semi-supervised learning approach. In Kentaro Inui, Jing Jiang, Vincent Ng, and Xiaojun Wan, editors, *Proceedings of the 2019 Conference on Empirical Methods in Natural Language Processing and the 9th International Joint Conference on Natural Language Processing, EMNLP-IJCNLP 2019, Hong Kong, China, November 3-7, 2019*, pages 2012–2023. Association for Computational Linguistics, 2019. 2

[35] Dong-Jin Kim, Jinsoo Choi, Tae-Hyun Oh, and In So Kweon. Image captioning with very scarce supervised data: Adversarial semi-supervised learning approach. In *Proceedings of the 2019 Conference on Empirical Methods in Natural Language Processing and the 9th International Joint Conference on Natural Language Processing (EMNLP-IJCNLP)*, pages 2012–2023, Hong Kong, China, Nov. 2019. Association for Computational Linguistics. 6

[36] Ryan Kiros, Ruslan Salakhutdinov, and Rich Zemel. Multi-modal neural language models. In *International conference on machine learning*, pages 595–603. PMLR, 2014. 2

[37] Ranjay Krishna, Yuke Zhu, Oliver Groth, Justin Johnson, Kenji Hata, Joshua Kravitz, Stephanie Chen, Yannis Kalantidis, Li-Jia Li, David A Shamma, et al. Visual genome: Connecting language and vision using crowdsourced dense image annotations. *International journal of computer vision*, 123(1):32–73, 2017. 13

[38] Girish Kulkarni, Visruth Premraj, Vicente Ordonez, Sagnik Dhar, Siming Li, Yejin Choi, Alexander C Berg, and Tamara L Berg. Babytalk: Understanding and generating simple image descriptions. *IEEE Transactions on Pattern Analysis and Machine Intelligence*, 35(12):2891–2903, 2013. 1, 2

[39] Zhenzhong Lan, Mingda Chen, Sebastian Goodman, Kevin Gimpel, Piyush Sharma, and Radu Soricut. Albert: A lite bert for self-supervised learning of language representations. In *International Conference on Learning Representations*, 2019. 3

[40] Kuang-Huei Lee, Xi Chen, Gang Hua, Houdong Hu, and Xiaodong He. Stacked cross attention for image-text matching. In *ECCV*, 2018. 2

[41] Mike Lewis, Yinhan Liu, Naman Goyal, Marjan Ghazvininejad, Abdelrahman Mohamed, Omer Levy, Veselin Stoyanov, and Luke Zettlemoyer. BART: Denoising sequence-to-sequence pre-training for natural language generation, translation, and comprehension. In *Proceedings of the 58th Annual Meeting of the Association for Computational Linguistics*. 2

[42] Christy Y Li, Xiaodan Liang, Zhiting Hu, and Eric P Xing. Hybrid retrieval-generation reinforced agent for medical image report generation. In *Proceedings of the 32nd International Conference on Neural Information Processing Systems*, pages 1537–1547, 2018. 6

[43] Guang Li, Linchao Zhu, Ping Liu, and Yi Yang. Entangled transformer for image captioning. In *Proceedings of the IEEE International Conference on Computer Vision*, pages 8928–8937, 2019. 2

[44] Siming Li, Girish Kulkarni, Tamara Berg, Alexander Berg, and Yejin Choi. Composing simple image descriptions using

web-scale n-grams. In *Proceedings of the Fifteenth Conference on Computational Natural Language Learning*, pages 220–228, 2011. 2

[45] Xiangyang Li and Shuqiang Jiang. Know more say less: Image captioning based on scene graphs. *IEEE Transactions on Multimedia*, 21(8):2117–2130, 2019. 2

[46] Xiujun Li, Xi Yin, Chunyuan Li, Pengchuan Zhang, Xiaowei Hu, Lei Zhang, Lijuan Wang, Houdong Hu, Li Dong, Furu Wei, et al. Oscar: Object-semantics aligned pre-training for vision-language tasks. In *European Conference on Computer Vision*, pages 121–137. Springer, 2020. 3

[47] Yuan Li, Xiaodan Liang, Zhiting Hu, and Eric P Xing. Hybrid retrieval-generation reinforced agent for medical image report generation. In *Advances in Neural Information Processing Systems 31*, pages 1530–1540. 2018. 1

[48] Yehao Li, Ting Yao, Yingwei Pan, Hongyang Chao, and Tao Mei. Pointing novel objects in image captioning. In *Proceedings of the IEEE/CVF Conference on Computer Vision and Pattern Recognition*, pages 12497–12506, 2019. 2

[49] Chin-Yew Lin. Rouge: A package for automatic evaluation of summaries. In *Text summarization branches out*, pages 74–81, 2004. 5

[50] Tsung-Yi Lin, Michael Maire, Serge Belongie, James Hays, Pietro Perona, Deva Ramanan, Piotr Dollár, and C Lawrence Zitnick. Microsoft COCO: Common objects in context. In *European conference on computer vision*, pages 740–755. Springer, 2014. 1, 4, 13

[51] Nelson F Liu, Matt Gardner, Yonatan Belinkov, Matthew E Peters, and Noah A Smith. Linguistic knowledge and transferability of contextual representations. In *Proceedings of the 2019 Conference of the North American Chapter of the Association for Computational Linguistics: Human Language Technologies*, pages 1073–1094, 2019. 4

[52] Siqi Liu, Zhenhai Zhu, Ning Ye, Sergio Guadarrama, and Kevin Murphy. Improved image captioning via policy gradient optimization of SPIDER. In *Proceedings of the IEEE international conference on computer vision*, pages 873–881, 2017. 2

[53] Yinhan Liu, Myle Ott, Naman Goyal, Jingfei Du, Mandar Joshi, Danqi Chen, Omer Levy, Mike Lewis, Luke Zettlemoyer, and Veselin Stoyanov. RoBERTa: A robustly optimized BERT pretraining approach. *arXiv Preprint*, arXiv 1907.11692, 2019. 2

[54] Yinhan Liu, Myle Ott, Naman Goyal, Jingfei Du, Mandar Joshi, Danqi Chen, Omer Levy, Mike Lewis, Luke Zettlemoyer, and Veselin Stoyanov. Roberta: A robustly optimized bert pretraining approach. 2019. 3

[55] Ilya Loshchilov and Frank Hutter. Fixing weight decay regularization in adam. 2018. 13

[56] Jiasen Lu, Dhruv Batra, Devi Parikh, and Stefan Lee. Vilbert: Pretraining task-agnostic visiolinguistic representations for vision-and-language tasks. In Hanna M. Wallach, Hugo Larochelle, Alina Beygelzimer, Florence d’Alché-Buc, Emily B. Fox, and Roman Garnett, editors, *Advances in Neural Information Processing Systems 32: Annual Conference on Neural Information Processing Systems 2019, NeurIPS 2019, 8-14 December 2019, Vancouver, BC, Canada*, pages 13–23, 2019. 3

[57] Jiasen Lu, Caiming Xiong, Devi Parikh, and Richard Socher. Knowing when to look: Adaptive attention via a visual sentinel for image captioning. In *Proceedings of the IEEE conference on computer vision and pattern recognition*, pages 375–383, 2017. 2

[58] Jiasen Lu, Jianwei Yang, Dhruv Batra, and Devi Parikh. Neural baby talk. In *Proceedings of the IEEE conference on computer vision and pattern recognition*, pages 7219–7228, 2018. 2

[59] Stephen Merity, Caiming Xiong, James Bradbury, and Richard Socher. Pointer sentinel mixture models. 2017. 2

[60] Tomáš Mikolov, Stefan Kombrink, Lukáš Burget, Jan Černocký, and Sanjeev Khudanpur. Extensions of recurrent neural network language model. In *2011 IEEE international conference on acoustics, speech and signal processing (ICASSP)*, pages 5528–5531. IEEE, 2011. 3

[61] Kishore Papineni, Salim Roukos, Todd Ward, and Wei-Jing Zhu. Bleu: a method for automatic evaluation of machine translation. In *Proceedings of the 40th annual meeting of the Association for Computational Linguistics*, pages 311–318, 2002. 5

[62] Karl Pearson. X. on the criterion that a given system of deviations from the probable in the case of a correlated system of variables is such that it can be reasonably supposed to have arisen from random sampling. *The London, Edinburgh, and Dublin Philosophical Magazine and Journal of Science*, 50(302):157–175, 1900. 8

[63] Matthew E Peters, Mark Neumann, Mohit Iyyer, Matt Gardner, Christopher Clark, Kenton Lee, and Luke Zettlemoyer. Deep contextualized word representations. In *Proceedings of NAACL-HLT*, pages 2227–2237, 2018. 3

[64] Di Qi, Lin Su, Jia Song, Edward Cui, Taroon Bharti, and Arun Sacheti. Imagebert: Cross-modal pre-training with large-scale weak-supervised image-text data. *arXiv preprint arXiv:2001.07966*, 2020. 3

[65] Alec Radford, Karthik Narasimhan, Tim Salimans, and Ilya Sutskever. Improving language understanding by generative pre-training. 2, 3

[66] Alec Radford, Jeffrey Wu, Rewon Child, David Luan, Dario Amodei, and Ilya Sutskever. Language models are unsupervised multitask learners. *OpenAI blog*, 1(8):9, 2019. 2, 3

[67] Colin Raffel, Noam Shazeer, Adam Roberts, Katherine Lee, Sharan Narang, Michael Matena, Yanqi Zhou, Wei Li, and Peter J. Liu. Exploring the limits of transfer learning with a unified text-to-text transformer. *Journal of Machine Learning Research*, 21(140):1–67, 2020. 2

[68] Shaoqing Ren, Kaiming He, Ross Girshick, and Jian Sun. Faster r-cnn: Towards real-time object detection with region proposal networks. In *Advances in neural information processing systems*, pages 91–99, 2015. 13

[69] Steven J Rennie, Etienne Marcheret, Youssef Mroueh, Jerret Ross, and Vaibhava Goel. Self-critical sequence training for image captioning. In *Proceedings of the IEEE Conference on Computer Vision and Pattern Recognition*, pages 7008–7024, 2017. 2, 4, 6

[70] Steven J Rennie, Etienne Marcheret, Youssef Mroueh, Jerret Ross, and Vaibhava Goel. Self-critical sequence training for

image captioning. In *Proceedings of the IEEE Conference on Computer Vision and Pattern Recognition*, pages 7008–7024, 2017. 6

[71] Steven J Rennie, Etienne Marcheret, Youssef Mroueh, Jerret Ross, and Vaibhava Goel. Self-critical sequence training for image captioning. In *Proceedings of the IEEE Conference on Computer Vision and Pattern Recognition*, pages 7008–7024, 2017. 13

[72] Anna Rohrbach, Lisa Anne Hendricks, Kaylee Burns, Trevor Darrell, and Kate Saenko. Object hallucination in image captioning. In *EMNLP*, 2018. 8

[73] Rico Sennrich, Barry Haddow, and Alexandra Birch. Neural machine translation of rare words with subword units. In *Proceedings of the 54th Annual Meeting of the Association for Computational Linguistics, ACL 2016, August 7-12, 2016, Berlin, Germany, Volume 1: Long Papers*. The Association for Computer Linguistics, 2016. 13

[74] Piyush Sharma, Nan Ding, Sebastian Goodman, and Radu Soricut. Conceptual captions: A cleaned, hypernymed, image alt-text dataset for automatic image captioning. In *Proceedings of the 56th Annual Meeting of the Association for Computational Linguistics (Volume 1: Long Papers)*, pages 2556–2565, 2018. 1, 4, 5, 13

[75] Rakshith Shetty, Marcus Rohrbach, Lisa Anne Hendricks, Mario Fritz, and Bernt Schiele. Speaking the same language: Matching machine to human captions by adversarial training. In *Proceedings of the IEEE International Conference on Computer Vision*, pages 4135–4144, 2017. 2

[76] Richard Socher and Li Fei-Fei. Connecting modalities: Semi-supervised segmentation and annotation of images using unaligned text corpora. In *2010 IEEE Computer Society Conference on Computer Vision and Pattern Recognition*, pages 966–973. IEEE, 2010. 2

[77] Weijie Su, Xizhou Zhu, Yue Cao, Bin Li, Lewei Lu, Furu Wei, and Jifeng Dai. ViL-bert: Pre-training of generic visual-linguistic representations. In *International Conference on Learning Representations*, 2020. 3

[78] Hao Tan and Mohit Bansal. LXMERT: learning cross-modality encoder representations from transformers. In Kentaro Inui, Jing Jiang, Vincent Ng, and Xiaojun Wan, editors, *Proceedings of the 2019 Conference on Empirical Methods in Natural Language Processing and the 9th International Joint Conference on Natural Language Processing, EMNLP-IJCNLP 2019, Hong Kong, China, November 3-7, 2019*, pages 5099–5110. Association for Computational Linguistics, 2019. 3

[79] Ashish Vaswani, Noam Shazeer, Niki Parmar, Jakob Uszkoreit, Llion Jones, Aidan N Gomez, Łukasz Kaiser, and Illia Polosukhin. Attention is all you need. In *Advances in neural information processing systems*, pages 5998–6008, 2017. 3, 5, 6, 7, 8, 14

[80] Ramakrishna Vedantam, C Lawrence Zitnick, and Devi Parikh. Cider: Consensus-based image description evaluation. In *Proceedings of the IEEE conference on computer vision and pattern recognition*, pages 4566–4575, 2015. 5

[81] Subhashini Venugopalan, Lisa Anne Hendricks, Marcus Rohrbach, Raymond Mooney, Trevor Darrell, and Kate Saenko. Captioning images with diverse objects. In *Proceedings of the IEEE conference on computer vision and pattern recognition*, pages 5753–5761, 2017. 2

[82] Oriol Vinyals, Alexander Toshev, Samy Bengio, and Dumitru Erhan. Show and tell: Lessons learned from the 2015 MSCOCO image captioning challenge. *IEEE transactions on pattern analysis and machine intelligence*, 39(4):652–663, 2016. 2

[83] Qingzhong Wang and Antoni B. Chan. Cnn+cnn: Convolutional decoders for image captioning. *arXiv 1805.09019*, 2018. 2

[84] Yufei Wang, Zhe Lin, Xiaohui Shen, Scott Cohen, and Garrison W Cottrell. Skeleton key: Image captioning by skeleton-attribute decomposition. In *Proceedings of the IEEE conference on computer vision and pattern recognition*, pages 7272–7281, 2017. 2

[85] Kelvin Xu, Jimmy Ba, Ryan Kiros, Kyunghyun Cho, Aaron Courville, Ruslan Salakhudinov, Rich Zemel, and Yoshua Bengio. Show, attend and tell: Neural image caption generation with visual attention. In *International conference on machine learning*, pages 2048–2057, 2015. 1, 2

[86] Xu Yang, Kaihua Tang, Hanwang Zhang, and Jianfei Cai. Auto-encoding scene graphs for image captioning. In *Proceedings of the IEEE Conference on Computer Vision and Pattern Recognition*, pages 10685–10694, 2019. 2

[87] Zhilin Yang, Zihang Dai, Yiming Yang, Jaime Carbonell, Russ R Salakhutdinov, and Quoc V Le. Xlnet: Generalized autoregressive pretraining for language understanding. In *Advances in neural information processing systems*, pages 5753–5763, 2019. 2

[88] Zhilin Yang, Ye Yuan, Yuxin Wu, William W Cohen, and Russ R Salakhutdinov. Review networks for caption generation. In D. Lee, M. Sugiyama, U. Luxburg, I. Guyon, and R. Garnett, editors, *Advances in Neural Information Processing Systems*, volume 29, 2016. 2

[89] Benjamin Z Yao, Xiong Yang, Liang Lin, Mun Wai Lee, and Song-Chun Zhu. I2t: Image parsing to text description. *Proceedings of the IEEE*, 98(8):1485–1508, 2010. 2

[90] Ting Yao, Yingwei Pan, Yehao Li, and Tao Mei. Exploring visual relationship for image captioning. In *Proceedings of the European conference on computer vision (ECCV)*, pages 684–699, 2018. 2

[91] Ting Yao, Yingwei Pan, Yehao Li, and Tao Mei. Hierarchy parsing for image captioning. In *Proceedings of the IEEE/CVF International Conference on Computer Vision*, pages 2621–2629, 2019. 2

[92] Yuanen Zhou, Meng Wang, Daqing Liu, Zhenzhen Hu, and Hanwang Zhang. More grounded image captioning by distilling image-text matching model. In *Proceedings of the IEEE/CVF Conference on Computer Vision and Pattern Recognition*, pages 4777–4786, 2020. 2

7. Supplementary material

In supplementary material, we provide experimental details and additional qualitative examples.

7.1. Additional implementation details

Image and Word Features. Following [3], we use a Faster R-CNN networks [68] with ResNet-101 [27] as a backbone to train on Visual Genome dataset [37], and we extract a 2048-dimensional feature vector for each object.

We use the Byte Pair Encoding (BPE) [73], which effectively incorporate sub-word information and is beneficial for dealing with out-of-vocabulary words. We employ learnable positional encoding and initialize token embedding from pretrained weights of GPT-2.

Architecture and Hyperparameters. We have 3 layers in the encoder and 12 layers in the decoder with 12 heads in each layer. The hidden size D in each layer is 768. We load the GPT-2 (small) pretrained weights, which has 117M parameters into the decoder. We use the learning rate of $1e^{-4}$ under XE loss and $1e^{-5}$ during the reinforcement learning. We train the models with the AdamW optimizer [55] and a batch size 25. The beam size is equal to 5. The threshold τ is tuned on the validation set for different training data.

7.2. Training Details

We train all the models in two steps. We first train the models with cross-entropy (XE) loss and then finetune them using reinforcement learning. The cross-entropy loss \mathcal{L}_{XE} is the traditional autoregressive classification loss

$$\mathcal{L}_{XE} = - \sum_{t=1}^T \log((w_t|w_{1:t-1})) \quad (7)$$

where $w_{1:T}$ represents the target ground truth sequence.

For reinforcement learning, we employ a variant of Self-Critical Sequence training [71]. Following [17], we sample L sentences, $\hat{w}_{1:T}^1, \dots, \hat{w}_{1:T}^L$, with beam search and use the mean reward from the L sentences as the baseline b . The gradient is

$$\nabla_{\theta} \mathcal{L}_{RL}(\theta) = -\frac{1}{k} \sum_{i=1}^L \left((r(\hat{w}_{1:T}^i) - b) \nabla_{\theta} \log p(\hat{w}_{1:T}^i) \right) \quad (8)$$

where $r(\cdot)$ represents the CIDEr-D reward.

7.3. More training dataset

Figure 7 shows other results obtained by training networks on the 5%, 10%, 20%, 50% and 100% data. VisualGPT outperforms other baseline models when we sample $\leq 20\%$ training data, highlighting its effectiveness on low data regimes.

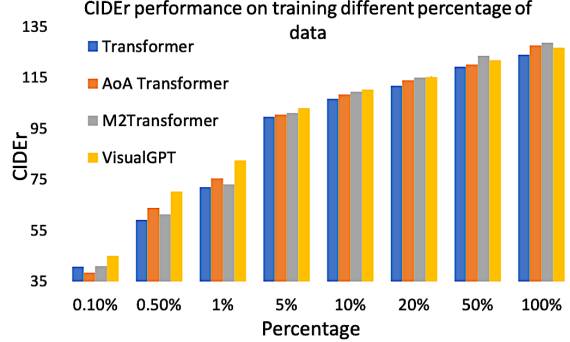


Figure 7. Evaluation on different percentage of data

Ablation	Decoder Layers	Decoder				
		B-1	B-4	M	R	C
0.1% Conceptual training						
Random init.	12	12.3	1.5	4.5	15.5	17.2
GPT2 init.	12	13.2	2.5	5.0	15.1	21.9
GPT2 init. + Meshed	12	11.9	2.6	4.9	15.4	24.0
GPT2 init. + AoA	12	11.8	2.8	4.6	13.9	20.5
Full VisualGPT	12	13.9	3.2	5.6	16.7	27.7
0.5% Conceptual training						
Random init.	12	12.8	3.0	4.7	15.7	25.4
GPT2 init.	12	16.2	3.8	6.5	18.3	35.6
GPT2 init. + Meshed	12	13.9	3.6	6.0	17.2	34.1
GPT2 init. + AoA	12	14.8	3.6	6.2	17.6	34.1
Full VisualGPT	12	15.4	4.1	6.6	18.4	37.4
1% Conceptual training						
Random init.	12	13.7	3.6	5.6	17.3	31.6
GPT2 init.	12	17.8	4.2	6.7	19.0	40.2
GPT2 init. + Meshed	12	15.4	3.9	6.5	17.9	39.1
GPT2 init. + AoA	12	15.3	3.9	6.4	17.9	38.5
Full VisualGPT	12	16.4	4.3	6.9	19.2	41.2

Table 8. Ablation studies on VisualGPT with different initialization, different cross-attention mechanisms trained on Conceptual subsets.

7.4. Conceptual Caption Ablations

We extend the ablation studies (Section 5.4 in main paper) of the effects of random initialization and pretrained GPT-2 weights to the Conceptual Caption dataset. The main results are shown in Table 8. Our VisualGPT consistently achieve best performance in most metrics, demonstrating its superiority over other methods.

7.5. Ablation study on τ of our SRAU

To evaluate the effect of different τ of our SRAU, we select the τ equals to 0, 0.1, 0.2 and 0.3 and test on the COCO [50] and Conceptual Caption[74] dataset. In Fig. 8

and 9 here, we show that $\tau > 0$ can outperform $\tau = 0$ in most cases. Meaning, SRAU is better than soft gating.

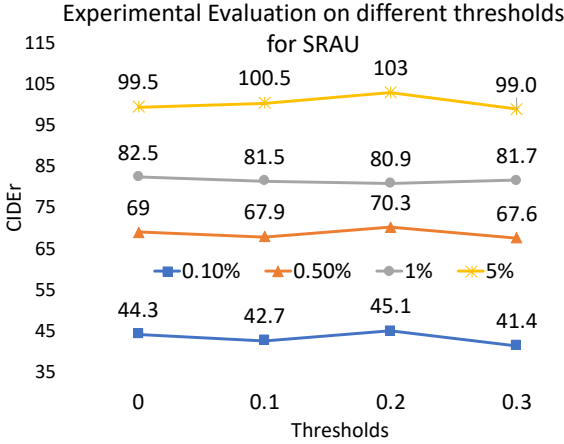


Figure 8. ablation study on different threshold τ on COCO dataset.

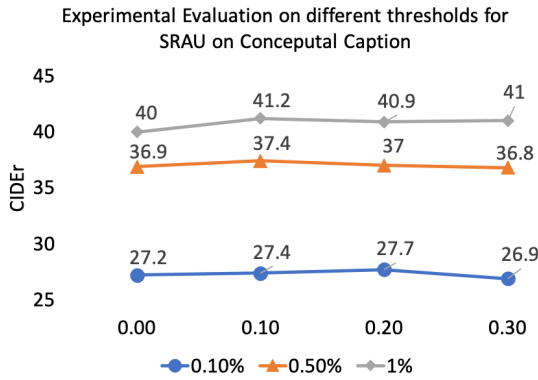


Figure 9. ablation study on different threshold τ on Conceptual Caption dataset.

7.6. Attention over Different types of words

We use the Spacy parser to detect the part-of-speech of words in captions and calculate the mean value of the visual attention score. The result is presented in Fig. 10. We found PoS that tend to visual content, like noun (0.71), verb (0.71) and adjective (0.72), have high visual attention scores, whereas linguistic PoS like pronoun (0.53), punctuation (0.58), and determiner (0.61) receive low attention.

7.7. More Qualitative Examples

In Figure 11, we provide more examples of visual attentions. Blue indicates high visual scores and red indicates low visual scores. We can observe that VisualGPT assigns higher scores to words like “steam engine”, “elephants”,

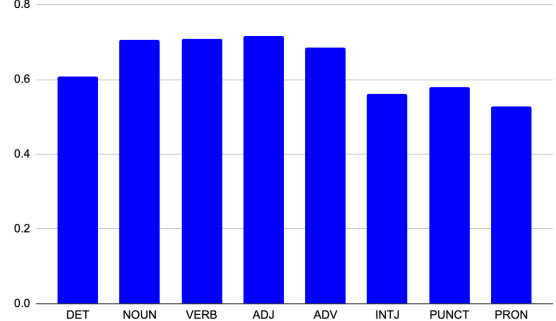


Figure 10. Attention Scores over different part-of-speech words

“horse”, “lush” and “cabinets”, and it assigns low visual scores to determiners and prepositions like “to” and “at”.

We also show some examples of generated captions by our VisualGPT and several strong baseline models including Transformer (3 layers) [79], \mathcal{M}^2 Transformer (3 layers) [17] and AoA Transformer [29] in the Table 9, Table 10 and Table 11. Overall, we can observe that our VisualGPT is able to describe the image content more accurately than the baseline models.

Image	Generated Captions	Ground Truth
	<p>Transformer: a woman riding some skis on skis \mathcal{M}^2 Transformer: a couple of skiers are standing near the snow AoA Transformer: a man with skis in the snow VisualGPT (ours): a group of people walk on a snowy mountain</p>	<p>GT1: the people are walking through snow in a wooded area GT2: two people wearing skis traveling through the snow GT3: a man is walking down a path covered in a snow GT4: a couple is skiing through the snowy woods GT5: a couple of people that are in a snowy field</p>
	<p>Transformer: a street that has some street in it \mathcal{M}^2 Transformer: a traffic light over a street light under a traffic light AoA Transformer: a street with people on a city street VisualGPT (ours): a street with tall signs and traffic signs</p>	<p>GT1: a yellow traffic light above a street next to houses GT2: a street scene of an intersection with a street light GT3: a stop light hanging over an intersection in a residential area GT4: a traffic signal at an intersection is suspended on wire GT5: a street intersection with a traffic light over it</p>
	<p>Transformer: some pizza are sitting on a plate \mathcal{M}^2 Transformer: a plate with food and a knife on it AoA Transformer: a plate of pizza on a table VisualGPT (ours): a plate of bread are served on a table</p>	<p>GT1: a batch of bread slices sitting on a plate GT2: a plate with some pieces of bread on it GT3: sliced french bread is on a plat that is lying on a table GT4: bread that is sitting on a plate that is on a table GT5: a white plate with lots topped with garlic bread</p>
	<p>Transformer: two tennis player playing tennis on the ball \mathcal{M}^2 Transformer: a tennis player about to hit a ball AoA Transformer: a baseball players on a game playing a game VisualGPT (ours): a tennis player hits a ball with a racket</p>	<p>GT1: a man holding a racquet on top of a tennis court GT2: a man with a tennis racket reaches for a ball GT3: a man with a tennis racket is running on a court GT4: a young man is playing a game of tennis GT5: a tennis player in a blue shirt runs toward a ball</p>
	<p>Transformer: a group of birds that are standing in the grass \mathcal{M}^2 Transformer: a flock of birds perched in a tree branch AoA Transformer: several giraffe are standing next to each trees VisualGPT (ours): a bird standing in the middle of a pond</p>	<p>GT1: a bird is perched a top a branch over a river GT2: a bird sits on a branch above a stream GT3: a bird on top of a tree branch over water GT4: a picture of an outside region that appears incredible GT5: a bird on a fallen branch in a body of water</p>

Table 9. Caption generated by our VisualGPT, Transformer, \mathcal{M}^2 Transformer and AoA Transformer on 0.1% MS COCO data split

Image	Generated Captions	Ground Truth
	<p>Transformer: several boats are sitting in the middle of a lake</p> <p>\mathcal{M}^2 Transformer: a boat filled with boats floating in the water</p> <p>AoA Transformer: an empty boat that has water and water</p> <p>VisualGPT (ours): a canal filled with boats in the water</p>	<p>GT1: a blue boat docked on a green lush shore</p> <p>GT2: a small marina with boats docked there</p> <p>GT3: a group of boats sitting together with no one around</p> <p>GT4: some boats parked in the water at a dock</p> <p>GT5: boats sitting around the side of a lake by a tree</p>
	<p>Transformer: pizza slices and pizza in a plate covered pizza</p> <p>\mathcal{M}^2 Transformer: people sitting at a table eating pizza and other salad</p> <p>AoA Transformer: two pizza eating a table with pizza on the table</p> <p>VisualGPT (ours): a group of pizza on a iron plate with toppings</p>	<p>GT1: a set of five pizzas sitting next to each other each with different toppings</p> <p>GT2: a handful of prepared pizzas sit next to each other</p> <p>GT3: five uncooked pizzas with a variety of different toppings</p> <p>GT4: five unbaked pizzas that include various types of cheeses</p> <p>GT5: five different pizzas are being prepared over a metal tray</p>
	<p>Transformer: a dog holding a frisbee in the water</p> <p>\mathcal{M}^2 Transformer: a dog holding a frisbee in a body of water</p> <p>AoA Transformer: a dog walking during a frisbee in a stone day</p> <p>VisualGPT (ours): a dog walking through the water with a frisbee</p>	<p>GT1: two dogs are playing on the beach catching a frisbee</p> <p>GT2: of two dogs only one may be the victor</p> <p>GT3: a dog catching a frisbee by another dog on a beach</p> <p>GT4: dog jumping up in the air to catch a frisbee in the summer time</p> <p>GT5: a dog jumping up into the air to catch a frisbee</p>
	<p>Transformer: a group of people taking a child in a in a building</p> <p>\mathcal{M}^2 Transformer: a group of people in an airport with their hands</p> <p>AoA Transformer: a picture of a young group of people standing for men</p> <p>VisualGPT (ours): a group of people standing around a tv</p>	<p>GT1: a group of men standing around a room</p> <p>GT2: some people are waiting in a long room</p> <p>GT3: people are standing in a room looking at a television screen</p> <p>GT4: a person sitting on a bench while the rest look somewhere else</p> <p>GT5: a man in red winter clothes sits on a bench with people behind him gather in front of a tv</p>
	<p>Transformer: an elephant eating a elephant has a elephant</p> <p>\mathcal{M}^2 Transformer: elephant with its trunk with their elephant with its trunk</p> <p>AoA Transformer: two elephants standing at a lot of trees</p> <p>VisualGPT (ours): three elephants standing next to some trees</p>	<p>GT1: two adult elephants are surrounding a baby elephant</p> <p>GT2: a baby elephant kneeling in front of two bigger elephants</p> <p>GT3: a baby elephant and it's parents eat fruit</p> <p>GT4: elephants eat fruit a baby elephant rummaging in the food</p> <p>GT5: a pair of adult elephants with a baby elephant eat from a pile of fruit</p>

Table 10. Caption generated by our VisualGPT, Transformer, \mathcal{M}^2 Transformer and AoA Transformer on 0.5% MS COCO data split

Image	Generated Captions	Ground Truth
	<p>Transformer: a man in a suit and a woman standing in a shop</p> <p>\mathcal{M}^2 Transformer: a man is standing in a shop with a people holding people</p> <p>AoA Transformer: a man is working on a bus in a</p> <p>VisualGPT (ours): a group of people standing at an airport with their luggage</p>	<p>GT1: several people are purchasing tickets at a bus station</p> <p>GT2: some people are checking in at the ticket counter somewhere in asia</p> <p>GT3: people waiting in line with luggage at a ticket counter</p> <p>GT4: people are standing near an airport ticket kiosk</p> <p>GT5: customers stand at a kiosk waiting for tickets</p>
	<p>Transformer: a bus that is parked in front of a building</p> <p>\mathcal{M}^2 Transformer: a couple of people walking down the side of a street</p> <p>AoA Transformer: a bus is parked in a city street</p> <p>VisualGPT (ours): a white and blue bus is parked on the side of a city street</p>	<p>GT1: people standing outside of a blue and white bus</p> <p>GT2: an image of a tour bus that is picking people up</p> <p>GT3: several people standing around buses and most wearing orange vests</p> <p>GT4: a public transit bus pulling up to pick up passengers</p> <p>GT5: a city bus at a stop waiting to pick up passengers</p>
	<p>Transformer: a blue and white airplane flying through a sky</p> <p>\mathcal{M}^2 Transformer: an air plane flying in the air</p> <p>AoA Transformer: a plane airplane flying down in the sky</p> <p>VisualGPT (ours): a plane is flying in the air over the trees</p>	<p>GT1: there 's and airplane in the sky flying over some trees</p> <p>GT2: a large plane is flying over a crowd of trees</p> <p>GT3: a aeroplane soaring high in the sky above the trees</p> <p>GT4: a passenger plane flies in the sky over a forest</p> <p>GT5: an airplane is seen flying over several trees</p>
	<p>Transformer: a white toilet sitting in a white bathroom next to a sink</p> <p>\mathcal{M}^2 Transformer: a cat sitting in the toilet</p> <p>AoA Transformer: a bathroom with a toilet and a sink</p> <p>VisualGPT (ours): a cat sitting on top of a bathroom sink</p>	<p>GT1: a cat climbing into a bathroom sink looking at someone</p> <p>GT2: a cat looks up as it stands in the bathroom sink</p> <p>GT3: a large cat stands inside of a clean bathroom sink</p> <p>GT4: cat is caught stepping in to the bathroom sink</p> <p>GT5: a cute kitty cat in the sink of a bathroom near a brush and other items</p>
	<p>Transformer: a little girl is eating a birthday cake</p> <p>\mathcal{M}^2 Transformer: a child and a child are sitting at a table with table with table</p> <p>AoA Transformer: two children sitting at a table with a laptop computer</p> <p>VisualGPT (ours): a woman and a girl sitting at a table with a birthday cake</p>	<p>GT1: a woman and child stand next to a table with cake on it</p> <p>GT2: a lady standing near the table with a baby is posing for the camera</p> <p>GT3: a woman stands beside a baby in a high chair a table is set with a birthday cake and champagne</p> <p>GT4: a woman setting up her house for a party</p> <p>GT5: a person standing next to a child in a booster seat</p>

Table 11. Caption generated by our VisualGPT, Transformer, \mathcal{M}^2 Transformer and AoA Transformer on 1% MS COCO data split

	GT: the large red flower is inside of a clear glass vase
	Ours a red vase of roses sitting on top of a glass attention 0.8 0.93 0.94 0.64 0.87 0.84 0.67 0.55 0.57 0.43 0.86
	GT: a tennis player jumps and hits a ball
	Ours a tennis player jumping on a tennis court holding a ball attention 0.7 0.77 0.75 0.72 0.67 0.64 0.89 0.79 0.74 0.6 0.76
	GT: a motorcycle parked next to a white building
	Ours a motorcycle parked next to a building attention 0.6 0.78 0.85 0.74 0.34 0.6 0.75
	GT: a small boats in a body of water
	Ours a large boat sits on a field with a lake attention 0.6 0.77 0.78 0.83 0.71 0.6 0.74 0.66 0.63 0.73
	GT: a kitchen with wooden cabinets a sink and a dish washer
	Ours a kitchen with a white cabinets and a sink attention 0.73 0.86 0.8 0.7 0.9 0.91 0.8 0.8 0.9
	GT: a train sitting under a display inside a building
	Ours a steam engine sitting in a display attention 0.69 0.84 0.79 0.8 0.7 0.6 0.83
	GT: two captive elephants stand bored behind the fake stone fence
	Ours elephants standing next to a stone fence attention 0.8 0.74 0.77 0.47 0.5 0.77 0.76
	GT: a white horse standing in a field on top of grass
	Ours a white horse grazing on a lush green field attention 0.67 0.75 0.83 0.74 0.65 0.66 0.85 0.8 0.77
	GT: a man in a restaurant smiling while holding up a camera
	Ours a man in a store looking at his camera attention 0.65 0.69 0.72 0.67 0.77 0.65 0.47 0.49 0.7
	GT: a man sitting on a bench next to a few bags
	Ours a young man holding a backpack on a bench attention 0.7 0.82 0.74 0.7 0.54 0.84 0.59 0.55 0.83

Figure 11. More examples of visual attention for each word in generated captions. High visual scores are in blue and low scores in red.